

Analytical Study of Free-Space Coupling of THz Radiation for a New Radioastronomy Receiver Concept

Gabriel Santamaría Botello¹, Kerlos Atia Abdalmalak¹, Maria-Theresa Schlecht², David González-Ovejero³, Florian Sedlmeir⁴, Harald G. L. Schwefel⁴, Stefan Malzer², Heiko Weber², Daniel Segovia-Vargas¹, Darragh McCarthy⁵, John Anthony Murphy⁵, Gottfried H. Döhler⁵, Luis-Enrique García Muñoz¹

¹Universidad Carlos III de Madrid, Spain.

²Friedrich-Alexander Erlangen-Nürnberg University, Germany.

³California Institute of Technology, USA.

⁴University of Otago, New Zealand.

⁵Maynooth University, Ireland.

legarcia@ing.uc3m.es

Abstract—In this paper, a scheme for coupling free-space THz radiation into a nonlinear whispering-gallery mode (WGM) resonator is presented. The purpose is to detect the weak THz radiation from the cosmic microwave background (CMB) by up-converting the signal into the optical domain via the nonlinearity of the medium. Such high-sensitivity receiver has theoretically shown capabilities towards photon counting at room temperature, however, it is critical to efficiently couple the THz radiation into the resonator. Therefore, by using the Schelkunoff-Waterman method (the so called T-matrix method) we perform an analytical evaluation of two different free-space coupling techniques: a free-space Gaussian beam, and a Gaussian beam incident in a silicon lens under total internal reflection. By comparing the excited modes in the resonator, the optimal parameters for each case are given.

Index Terms—Cosmic microwave background, THz, photon-counting, whispering-galley mode, T-matrix.

I. INTRODUCTION

The measurement of the so called B-mode polarization component of the cosmic microwave background would allow the indirect detection of primordial gravitational waves, providing a definitive test of inflationary paradigm [1]. Thus, this is a high interest area where high-sensitivity photon-counting receivers at sub-THz and THz frequencies are needed. A receiver scheme which has theoretically shown capabilities towards photon-counting sensitivity at room-temperature is the nonlinear parametric up-conversion of the THz signal into the optical domain via the second-order nonlinear response $\chi^{(2)}$ of a dielectric [2]. By mixing the THz signal with an optical pump inside a nonlinear dielectric, sidebands are created through sum frequency generation (SFG) and difference frequency generation (DFG) [3]. Since the sidebands are in the optical domain, they can be detected with currently available high-sensitivity optical detectors. In order to achieve an efficient nonlinear interaction of the THz signal and the optical pump inside the medium, high field intensities are required. A travelling-wave resonator made of a nonlinear material is

therefore suitable because it can considerably enhance the intra-cavity field intensity in continuous wave (CW) operation. A conceptual scheme of the receiver is depicted in Fig. 1. A whispering-gallery mode is excited inside a resonator made of LiNbO_3 for each frequency (THz signal, optical pump and up-converted optical signal), whose angular velocities must be equal in order to fulfill the phase-matching condition [4]. A prism is used to couple-in the pump coming from a laser and to couple-out the up-converted signal which is then detected by an optical receiver. Total internal reflection (TIR) evanescent field arising from the prism interface allows the coupling. Dielectric waveguides have shown to be suitable for coupling the THz signal into the resonator since they have a relatively well mode overlapping with the WGM evanescent field [5], [6], however bulky interfaces including a horn antenna and transitions are required to couple free-space THz field to the dielectric waveguide. In this paper, we evaluate the coupling given by the TIR field arising when a THz Gaussian beam is incident into a semi-spherical silicon lens beyond the critical angle, and compare this with the direct coupling of the Gaussian beam without lens. This lens coupling mechanism emulates the prism used for optical frequencies. The analysis is carried out by computing the excited fields inside the resonator due to the incident field, by means of the Schelkunoff-Waterman method.

The paper is structured as follows: In Section II we briefly discuss the mathematical formulation of the problem and compute the resonator's internal field matrix. In Section III, the free-space and TIR Gaussian beam field wave expansions are computed. Finally, we present results of the analysis in Section IV and conclusions in Section V.

II. MATHEMATICAL FORMULATION

In order to study the coupling of the field into the resonator, we reduce the system to a scattering problem, with

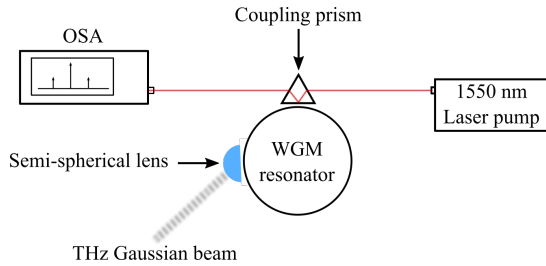


Fig. 1. General receiver scheme. The laser pump and up-converted signal are coupled through a prism via frustrated total internal reflection. A THz Gaussian beam is coupled as a WGM inside the resonator by means of a semi-spherical lens.

the resonator being the scatterer and the free-space or TIR Gaussian beam being the incident field. This assumes the resonator resonance is not affected by the presence of the semi-spherical which is a good approximation for confined WGM as the ones we are dealing with [8]. Following [7], we use the equivalence principle to remove the scatterer and substitute it by equivalent surface primary sources $\mathbf{J}^+ = \hat{\mathbf{a}}_n \times (\mathbf{H}^i + \mathbf{H}^s)$ and $\mathbf{M}^+ = \hat{\mathbf{a}}_n \times (\mathbf{E}^i + \mathbf{E}^s)$, with $\hat{\mathbf{a}}_n$ being the normal vector to the surface of the scatterer, \mathbf{E}^i , \mathbf{H}^i being the incident electric and magnetic fields respectively, and \mathbf{E}^s , \mathbf{H}^s being the scattered electric and magnetic fields respectively. Such sources radiate the field \mathbf{E}^s , \mathbf{H}^s outside the body, and $-\mathbf{E}^i$, $-\mathbf{H}^i$ inside of it. Therefore, evaluating the observation point \mathbf{r} inside the resonator, we have:

$$\begin{aligned} \nabla \times \oint_S \mathbf{M}^+(\mathbf{r}') \cdot \bar{\mathbf{G}}(\mathbf{r}, \mathbf{r}') dS' \\ - \nabla \times \nabla \times \oint_S \frac{\mathbf{J}^+(\mathbf{r}')}{i\omega\epsilon_0} \cdot \bar{\mathbf{G}}(\mathbf{r}, \mathbf{r}') dS' = -\mathbf{E}^i(\mathbf{r}) \end{aligned} \quad (1)$$

where we have assumed $\exp(i\omega t)$ harmonic time dependence, S is the resonator surface and $\bar{\mathbf{G}}(\mathbf{r}, \mathbf{r}') = \bar{\mathbf{I}}g(\mathbf{r}, \mathbf{r}')$, being $g(\mathbf{r}, \mathbf{r}')$ the free-space Green's function and $\bar{\mathbf{I}}$ the unit dyadic. Now, we expand $\bar{\mathbf{G}}(\mathbf{r}, \mathbf{r}')$, \mathbf{E}^i and the internal field of the original problem \mathbf{E}^t , \mathbf{H}^t in vector spherical harmonics which form a complete basis [9]–[11] as:

$$\bar{\mathbf{G}}(\mathbf{r}, \mathbf{r}') = i\kappa_0 \sum_{n,m,\sigma} (-1)^m \mathbf{F}_{\sigma-mn}^{(3)}(\kappa_0, \mathbf{r}') \mathbf{F}_{\sigma-mn}^{(1)}(\kappa_0, \mathbf{r}) \quad (2)$$

$$\mathbf{E}^i(\mathbf{r}) = \kappa_0 \sqrt{\eta_0} \sum_{n,m,\sigma} a_{\sigma mn} \mathbf{F}_{\sigma mn}^{(1)}(\kappa_0, \mathbf{r}) \quad (3)$$

$$\mathbf{E}^t(\mathbf{r}) = \kappa_1 \sqrt{\eta_1} \sum_{n,m,\sigma} c_{\sigma mn} \mathbf{F}_{\sigma mn}^{(1)}(\kappa_1, \mathbf{r}) \quad (4)$$

where κ_0, η_0 and κ_1, η_1 are the wavenumber and impedance of vacuum and resonator respectively. The corresponding magnetic fields can be obtained by changing $\sigma \rightarrow 3 - \sigma$ and multiplying by $-i/\eta$. In the above equations, the summation $\sum_{n,m,\sigma} \equiv \sum_{n=1}^{\infty} \sum_{m=-n}^n \sum_{\sigma=1}^2$ is truncated until some $n = N$. The indices n and m determine the radial and azimuthal

behavior of the mode respectively, and $\sigma = 1$ represents TE modes, while $\sigma = 2$ represents TM modes. The mathematical expressions of $\mathbf{F}_{\sigma mn}^{(1,3)}(\kappa_0, \mathbf{r})$ are given in [11]. Considering that boundary conditions must hold, i.e., $\mathbf{J}^+ = \hat{\mathbf{a}}_n \times \mathbf{H}^t$ and $\mathbf{M}^+ = \hat{\mathbf{a}}_n \times \mathbf{E}^t$, and applying orthogonality properties of the functions $\mathbf{F}_{\sigma mn}^{(1,3)}(\kappa_0, \mathbf{r})$ over any spherical surface inside the resonator whose volume contains a homogeneous medium, we finally get a $2N \times 2N$ system of equations:

$$\begin{aligned} a_{1uv} = \sum_{n,m} \left(L_{mnuv}^{2,1} + \frac{\eta_0}{\eta_2} L_{mnuv}^{1,2} \right) c_{1mn} \\ + \left(L_{mnuv}^{2,2} + \frac{\eta_0}{\eta_2} L_{mnuv}^{1,1} \right) c_{2mn} \end{aligned} \quad (5)$$

$$\begin{aligned} a_{2uv} = \sum_{n,m} \left(L_{mnuv}^{1,1} + \frac{\eta_0}{\eta_2} L_{mnuv}^{2,2} \right) c_{1mn} \\ + \left(L_{mnuv}^{1,2} + \frac{\eta_0}{\eta_2} L_{mnuv}^{2,1} \right) c_{2mn} \end{aligned} \quad (6)$$

with,

$$L_{mnuv}^{\sigma s} = K_u \oint_S \hat{\mathbf{a}}_n \cdot \left[\mathbf{F}_{\sigma-mn}^{(3)}(\kappa_0, \mathbf{r}') \times \mathbf{F}_{smn}^{(1)}(\kappa_1, \mathbf{r}) \right] dS' \quad (7)$$

where

$$K_u = \frac{i\kappa_0 \kappa_1 (-1)^u}{\sqrt{\eta_0/\eta_2}} \quad (8)$$

Such system of equations can be solved for the internal field coefficients $c_{\sigma mn}$ given the incident field coefficients a_{suv} . WGM resonators are axisymmetric (spheres, discs, rings, etc), and in such case $L_{mnuv}^{\sigma s} = 0$ for $u \neq m$ which reduces considerably the computation time of the matrix of the system. Surface integral of Eq. (7) must be solved numerically, however it simplifies to a 1-dimensional one for axisymmetric resonators. In the case the scatterer is a sphere, $L_{mnuv}^{\sigma s} = 0$ for $(u, v) \neq (m, n)$ and the resultant matrix is diagonal.

III. INCIDENT FIELD EXPANSIONS

We take into consideration two cases of interest: A Gaussian beam in free space and under TIR when changing from the dielectric lens medium, to vacuum. In each case, the fields will be expanded in a superposition of plane waves, and each one of these will be expanded in vector spherical harmonics. This way the total incident field coefficients a_{suv} are determined.

A. Free-space Gaussian Beam

Consider a Gaussian beam propagating in the $+z$ direction, with its focus in the origin of the coordinate system, beam waist w_0 , and linear polarization in the x axis. The x component of the field E_x in the plane $z = 0$ has the form [12]:

$$E_x = E_0 \exp\left(-\frac{x^2 + y^2}{w_0^2}\right) \quad (9)$$

whose two dimensional Fourier transform in the plane xy (or plane wave spectrum) is

$$\mathcal{F}_{xy}[E_x] = \pi w_0^2 E_0 \exp\left[-\frac{w_0^2}{4}(\kappa_x^2 + \kappa_y^2)\right] \quad (10)$$

so we can obtain the field as a continuous superposition of plane waves, i.e.,

$$E_x(\mathbf{r}) = \frac{w_0^2 E_0}{4\pi} \int_{-\infty}^{\infty} \int_{-\infty}^{\infty} \exp\left[-\frac{w_0^2}{4}(\kappa_x^2 + \kappa_y^2)\right] \cdot \exp(i\boldsymbol{\kappa} \cdot \mathbf{r}) d\kappa_x d\kappa_y \quad (11)$$

where $\boldsymbol{\kappa} = \kappa_x \hat{\mathbf{a}}_x + \kappa_y \hat{\mathbf{a}}_y + \kappa_z \hat{\mathbf{a}}_z$ and $\kappa_z = \sqrt{\kappa_0^2 - \kappa_x^2 - \kappa_y^2}$. The surface integral of Eq. (11) spans over an infinite domain (κ_x, κ_y) . However, for $\kappa_x^2 + \kappa_y^2 > \kappa_0^2$, the spectrum has small values and such fraction of evanescent waves can be neglected [12]. Therefore we can perform the integration over a circle of radius κ_0 in the plane (κ_x, κ_y) . In order to satisfy Maxwell's equations, the field must also have a z component given by the relation $\mathbf{E} \cdot \boldsymbol{\kappa} = 0$, thus

$$\mathbf{E}(\mathbf{r}) = \left(\hat{\mathbf{a}}_x - \frac{\kappa_x}{\kappa_z} \hat{\mathbf{a}}_z \right) E_x(\mathbf{r}) \quad (12)$$

The total field can be evaluated by changing variables in the area integral of Eq. (11) to express $\boldsymbol{\kappa}$ in spherical coordinates, yielding

$$\mathbf{E}(\mathbf{r}) = \frac{w_0^2 E_0 \kappa_0^2}{8\pi} \int_0^{2\pi} \int_0^{\pi/2} \left(\hat{\mathbf{a}}_x - \frac{\cos \varphi}{\cos \theta} \hat{\mathbf{a}}_z \right) \sin 2\theta \cdot \exp\left[-\left(\frac{w_0}{2} \kappa_0 \sin \theta\right)^2\right] \exp(i\boldsymbol{\kappa}(\theta, \varphi) \cdot \mathbf{r}) d\theta d\varphi \quad (13)$$

with,

$$\boldsymbol{\kappa}(\theta, \varphi) = \kappa_0 (\sin \theta \cos \varphi \hat{\mathbf{a}}_x + \sin \theta \sin \varphi \hat{\mathbf{a}}_y + \cos \theta \hat{\mathbf{a}}_z) \quad (14)$$

The expression for the beam with the focus in an arbitrary position \mathbf{r}_0 can be obtained replacing $\mathbf{r} \rightarrow \mathbf{r} - \mathbf{r}_0$ in Eq. (13).

The expansion coefficients $b_{\sigma mn}$ of a plane wave $\mathbf{A} \exp[i\boldsymbol{\kappa}(\theta, \varphi) \cdot \mathbf{r}]$ in vector spherical harmonics are given by [11]:

$$b_{\sigma mn} = \frac{2\sqrt{\pi}(-1)^{m+1}}{\kappa_0 \sqrt{\eta_0}} i \mathbf{A} \cdot \mathbf{K}_{\sigma mn}^*(\theta, \varphi) \quad (15)$$

where, $\mathbf{K}_{\sigma mn}^*(\theta, \varphi)$ is the conjugated of the far-field pattern function composed by Legendre polynomials given in [11]. Eq. (15) is valid for complex angles θ, φ allowing the representation of evanescent plane waves. Finally, expanding each plane wave of Eq. (13) into a series analogous to Eq. (3) with the coefficients given by Eq. (15), the resulting coefficients of the total beam are determined by the following numerical integral:

$$a_{\sigma mn} = C_m \int_0^{2\pi} \int_0^{\pi/2} \left(\hat{\mathbf{a}}_x - \frac{\cos \varphi}{\cos \theta} \hat{\mathbf{a}}_z \right) \cdot \mathbf{K}_{\sigma mn}^*(\theta, \varphi) \cdot \sin 2\theta \exp\left[-\left(\frac{w_0}{2} \kappa_0 \sin \theta\right)^2\right] d\theta d\varphi \quad (16)$$

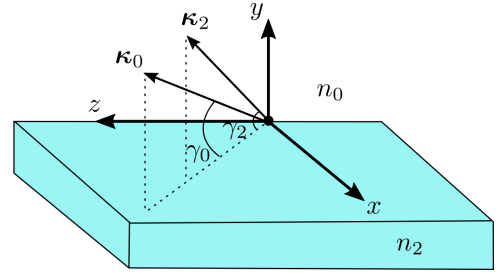


Fig. 2. Incidence of a Gaussian beam from silicon (n_2) to vacuum (n_0)

with

$$C_m = \frac{i(-1)^{m+1} w_0^2 E_0 \kappa_0}{4\sqrt{\pi} \sqrt{\eta_0}} \quad (17)$$

In order to represent an arbitrarily oriented Gaussian beam, Eq. (16) can still be used considering the integral sweeps over the θ and φ angles with respect to the beam's axis. However, the function $\mathbf{K}_{\sigma mn}^*$ must be evaluated at the actual angles $\theta'(\theta, \varphi)$ and $\varphi'(\theta, \varphi)$ with respect to the fixed coordinate system, and the unitary vectors must be evaluated in such coordinate system as well.

B. Gaussian beam under TIR

Consider the dielectric-air interface placed in the $y = 0$ plane, and a Gaussian beam arbitrarily oriented coming from the dielectric to the interface (see Fig. 2). From the arbitrarily oriented form of Eq. (16) we apply Snell's laws to each plane wave coming from silicon determined by $\mathbf{K}_{\sigma mn}^*(\theta'(\theta, \varphi), \varphi'(\theta, \varphi))$ and the wavevector $\boldsymbol{\kappa}_2$ forming an angle γ_2 with the interface. Then, the plane wave is refracted to vacuum with wavevector $\boldsymbol{\kappa}_2$ forming an angle γ_0 with the interface which is determined by

$$\gamma_0 = \arccos\left(\frac{n_2}{n_0} \cos \gamma_2\right) \quad (18)$$

where $\gamma_2 = \arcsin(\sin \theta' \cos \varphi')$ and must be real. γ_0 can be complex if the specific plane wave is under TIR. In any case, the transmitted wave vector is given by

$$\boldsymbol{\kappa}_0 = \cos \gamma_0 \hat{\boldsymbol{\rho}} + \sin \gamma_0 \hat{\mathbf{a}}_y = \kappa_{0x} \hat{\mathbf{a}}_x + \kappa_{0y} \hat{\mathbf{a}}_y + \kappa_{0z} \hat{\mathbf{a}}_z \quad (19)$$

with $\hat{\boldsymbol{\rho}} = \boldsymbol{\kappa}_2 - (\boldsymbol{\kappa}_2 \cdot \hat{\mathbf{a}}_y) \hat{\mathbf{a}}_y$ being the real normal vector to $\hat{\mathbf{a}}_y$ and parallel to the plane of incidence. From that, the transmitted plane wave angles (θ'_0, φ'_0) are

$$\theta'_0 = \arccos\left(\frac{\kappa_{0z}}{\sqrt{\kappa_{0x}^2 + \kappa_{0y}^2 + \kappa_{0z}^2}}\right) \quad (20)$$

$$\varphi'_0 = \arccos\left(\frac{\kappa_{0x}}{\sqrt{\kappa_{0x}^2 + \kappa_{0y}^2}}\right) \quad (21)$$

$$\varphi'_0 = \arcsin\left(\frac{\kappa_{0y}}{\sqrt{\kappa_{0x}^2 + \kappa_{0y}^2}}\right) \quad (22)$$

The angle φ'_0 must be simultaneously determined from multi-valuated Eqs. (21) and (22). θ'_0 and φ'_0 are in general complex and must be substituted in $\mathbf{K}_{\sigma mn}^*(\theta'_0, \varphi'_0)$ from Eq. (16) after multiplying by the Fresnel coefficients for each polarization. Note that (θ'_0, φ'_0) depend on γ_2 , which depend on (θ', φ') which is in turn a function of the integration variables (θ, φ) according to arbitrary rotation of the beam. The dielectric-air interface can be translated a distance d in the $-y$ axis to some point $y = -d$ by substituting $\mathbf{r} \rightarrow \mathbf{r} + d\hat{\mathbf{a}}_y$ in Eq. (13) which leads to a multiplication factor $\exp[i\kappa_{0y}(\theta'_0, \varphi'_0)d]$ in Eq. (16).

IV. RESULTS

In this section, we study the coupling in an spherical resonator made of sapphire with refractive index $n_r = 3.01$. The radius of the sphere is $R_a = 2.5$ mm and is being excited at its resonance frequency for a fundamental TE WGM of mode number $m, n = 8, 8$. The resonance frequency is determined by the characteristic equation [8].

$$\begin{aligned} \frac{d}{dr}[rj_n(n_r\kappa_0r)] \Big|_{r=R_a} h_n^{(1)}(\kappa_0R_a) \\ = \frac{d}{dr}[rh_n^{(1)}(\kappa_0r)] \Big|_{r=R_a} j_n(n_r\kappa_0R_a) \end{aligned} \quad (23)$$

where $j_n(x)$ is the spherical Bessel function $h_n^{(1)}(x)$ is the spherical Hankel function of first kind. The solution of this equation for the mode $n = 8$ is a complex frequency whose imaginary part accounts for the radiation and absorption losses and whose real part results $f = 73.28$ GHz. Since we are dealing with a sphere, the internal field matrix, and its inverse are diagonals as was shown in Section II. Therefore, the internal field coefficients can be determined with the simple relation

$$c_{\sigma mn} = D_{mn}^{-1} a_{\sigma mn} \quad (24)$$

where D_{mn} are the diagonal elements of the matrix. Due to the strong resonance of modes $n = 8$, the elements D_{mn}^{-1} act as filter of such modes for the given frequency as shown in Fig. 3. Therefore, is sufficient to compare the strength of the desired mode in the expansion of the different incident fields.

A. Free-space Gaussian beam coupling

Fig. 4 shows the coupling scheme of a free-space Gaussian beam traveling in x direction with polarization in z direction. The beam's focus and the center of the sphere are separated a distance h in a plane which is transversal to the beam. Figure 5 shows there is an optimal distance h where the coupling to mode $m, n = 8, 8$ is maximized. This distance agrees with the approximation given in [13] and is physically linked to the Van de Hulst's localization principle [14]. The beam waist is $w_0 = \lambda_0$, but an iterative study also showed that for the same beam power, the magnitude of a_{188} decrease monotonically by increasing the beam waist w_0 or by translating the focus

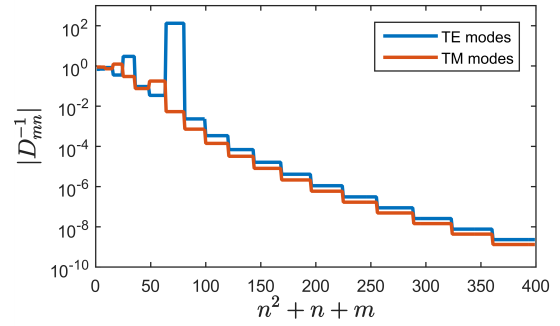


Fig. 3. Magnitude of the diagonal elements of the inverse matrix as a function of the mode m, n

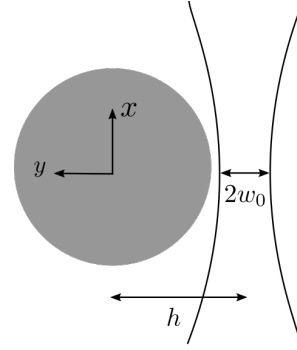


Fig. 4. Free-space Gaussian Beam coupling

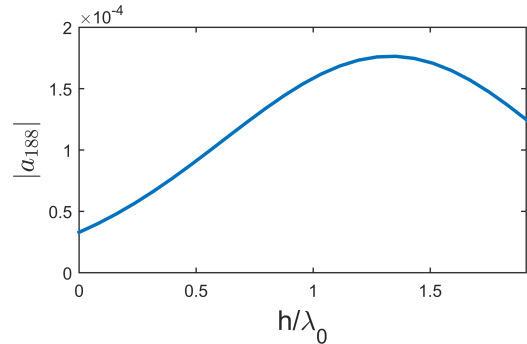


Fig. 5. Magnitude of the Gaussian beam mode TE $m, n = 8, 8$ as a function of the distance h from the focus to the center of the sphere

point towards the x direction. Fig 6 shows the resulting excited field inside the resonator is a WGM $m, n = 8, 8$ with a field intensity higher than the incoming Gaussian beam's electric field amplitude of 1V/m.

B. TIR Gaussian beam coupling

A similar study has been done for the TIR case. A Gaussian beam with waist radius $w_0 = \lambda_0$ propagates from a silicon medium ($n_2 = 3.42$) to the silicon-air interface which is at a distance $g = 0.05\lambda_0$ from the surface of the resonator. Different incidence angles were evaluated to obtain the curve shown in Fig. 7. It can be seen an optimal angle exists at $\gamma_2 = 32.6^\circ$, which is close to the angle a plane wave must

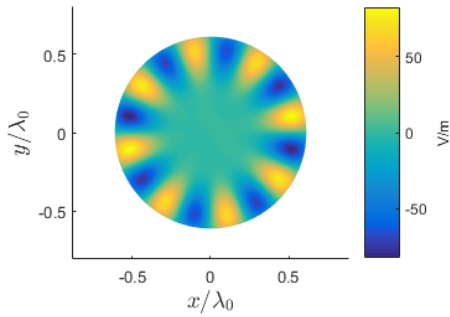


Fig. 6. Electric field excited inside the resonator with the free-space Gaussian beam coupling in the plane $z = 0$. The beam has an electric field amplitude of 1 V/m.

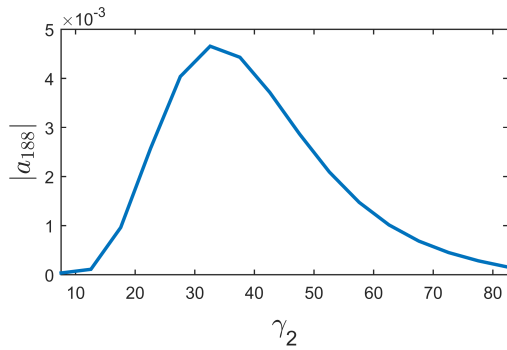


Fig. 7. Dependence of the coefficient $|a_{188}|$ with the incidence angle of the beam

propagate with in order to phase-match the WGM evanescent field with the TIR evanescent field:

$$\gamma_{2_{approx}} = \arcsin\left(\frac{cm}{2\pi fn_2 R_a}\right) \approx 37.58^\circ \quad (25)$$

As in the previous section, increasing the beam waist while keeping the same power, or moving the focus point along the direction of propagation, only decreases the coupling strength. Note that the coefficient a_{188} is about 25 time higher for the TIR case than for the free-space case which means the lens is suitable for free-space coupling. Fig 8 shows the excited WGM is again the desired $m, n = 8, 8$ mode with a much higher amplitude than in the free-space Gaussian beam case. In order to compare with the same incoming power, the beam's electric field amplitude has been scaled accordingly to $1/\sqrt{n_2}$ V/m.

V. CONCLUSION

The mathematical framework of the Schelkunoff-Waterman method has been used to study the excited internal field of a spherical resonator for a given incident field structure. Two free-space different excitations configurations have been compared: free-space Gaussian beam, and Gaussian beam incident in a silicon lens under TIR. The latter showed a considerable improvement in the coupling strength of a particular mode, although the influence of the lens in the resonance was

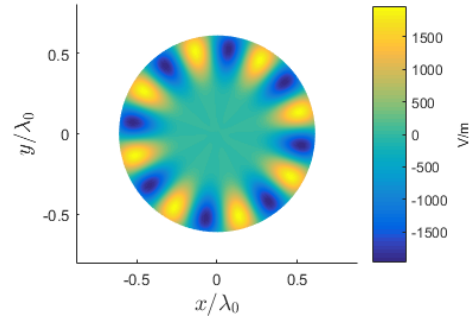


Fig. 8. Electric field excited inside the resonator with the TIR Gaussian beam coupling in the plane $z = 0$. The beam has an electric field amplitude of $1/\sqrt{n_2}$ V/m.

neglected. As a better approximation we can compute the multiple reflections appearing between the lens planar interface and the resonator. This approach is suitable to quickly analyze the performance of different incident field configurations and other resonator geometries, although numerical inaccuracies arise for high permittivities or highly non-spherical bodies.

ACKNOWLEDGMENT

This work has been financially supported by “DiDaCTIC: Desarrollo de un sistema de comunicaciones inalámbrico en rango THz integrado de alta tasa de datos”, TEC2013-47753-C3, CAM S2013/ICE-3004 “DIFRAGEOS” projects, “Proyecto realizado con la Ayuda Fundación BBVA a Investigadores y Creadores Culturales 2016.” and “Estancias de movilidad de profesores PRX16/00021”.

REFERENCES

- [1] A. G. Polnarev, *Polarization and Anisotropy Induced in the Microwave Background by Cosmological Gravitational Waves*, *Sov. Astron.* 29, 607, 1985
- [2] A.B Matsko, et al, *Sensitivity of THz photonic receivers*, *Physical Review A* 77, 043812, 2008.
- [3] P.E. Powers, *Fundamentals of Nonlinear Optics*. CRC Press. 2011
- [4] R. W. Boyd, *Nonlinear Optics*. 2nd ed. 2003
- [5] Brent E. Little, *Analytic Theory of Coupling from Tapered Fibers and Half-Blocks into Microsphere Resonators*, *Journal of Lightwave Technology*. 17, 4, 1999
- [6] A. Rivera-Lavado et al., *Dielectric Rod Waveguide Antenna as THz Emitter for Photomixing Devices*, *IEEE Transactions on Antennas and Propagation*, Vol. 63, 3, 2015.
- [7] P. Barber, C. Yeh, *Scattering of electromagnetic waves by arbitrarily shaped dielectric bodies*, *Applied Optics*. 14, 12, 1975
- [8] A. N. Oraevsky, *Whispering-Gallery waves*, *Quantum Electronics*, Vol. 32, No. 5, pp.377-400, 2002.
- [9] Stratton J. A., *Electromagnetic Theory*, McGraw-Hill, New York, 1941.
- [10] P. M. Morse, H. Feshbach, *Methods of Theoretical Physics*, McGraw-Hill, New York, 1953.
- [11] J. E. Hansen, *Spherical near-field antenna measurements*, IEE Electromagnetic Waves Series, 26.
- [12] E. E. M. Khaled, *Scattered and Internal Intensity of a Sphere Illuminated with a Gaussian Beam*, *IEEE Transactions on Antennas and Propagation*, Vol. 41, No. 3, 1993.
- [13] James A. Lock, *Excitation Efficiency of a Morphology-Dependent Resonance by a Focused Gaussian Beam*, *J. Opt. Soc. Am.* Vol. 15, No. 12, 1998.
- [14] H. C. van de Hulst, *Light scattering by small particles*, Dover Publications.